Spin-Orbit Dimers and Noncollinear Phases in d^{1} Cubic Double Perovskites

Judit Romhányi, Leon Balents, and George Jackeli

Phys. Rev. Lett. **118**, 217202 — Published 26 May 2017

DOI: 10.1103/PhysRevLett.118.217202

Spin-Orbit Dimers and Non-Collinear Phases in d^1 Cubic Double Perovskites

Judit Romhányi,[1,2] Leon Balents,[3] and George Jackeli[1,4,*]

[1] *Max Planck Institute for Solid State Research, Heisenbergstrasse 1, D-70569 Stuttgart, Germany*
[2] *Okinawa Institute of Science and Technology Graduate University, Onna-son, Okinawa 904-0395, Japan*
[3] *Kavli Institute for Theoretical Physics, University of California, Santa Barbara, CA 93106, USA*
[4] *Institute for Functional Matter and Quantum Technologies, University of Stuttgart, Pfaffenwaldring 57, D-70569 Stuttgart, Germany*

(Dated: March 30, 2017)

We formulate and study a spin-orbital model for a family of cubic double perovskites with d^1 ions occupying a frustrated fcc sublattice. A variational approach and a complimentary analytical analysis reveal a rich variety of phases emerging from the interplay of Hund's and spin-orbit couplings (SOC). The phase digram includes non-collinear ordered states, with or without net moment, and, remarkably, a large window of a non-magnetic disordered spin-orbit dimer phase. The present theory uncovers the physical origin of the unusual amorphous valence bond state experimentally suggested for Ba_2BMoO_6 (B=Y,Lu), and predicts possible ordered patterns in Ba_2BOsO_6 (B=Na,Li) compounds.

PACS numbers: 75.10.Jm, 75.30.Et

Conventionally, frustration, low dimensionality and low spin are the key attributes of emerging novel quantum ground states. In the quest to realize a quantum spin liquid, a state of spins possessing massive quantum entanglement and lacking magnetic order, researchers have extensively studied Mott insulators with antiferromagnetic (AF) interactions on geometrically frustrated triangular, kagome, hyper-kagome and pyrochlore lattices [1, 2]. Another route to frustration in Mott insulators with unquenched angular momentum is provided by orbital degrees of freedom. The directional character of degenerate d-orbitals may frustrate the magnetic interactions even on bipartite lattices, and lead to a plethora of emergent phases with unusual spin patterns [3, 4] or without long-range spin/orbital order [5–10].

In $4d$ and $5d$ transition metal compounds, the enhanced SOC, compared to $3d$ systems, fully or partly lifts the local degeneracy of a d-shell. When degeneracy is fully lifted, e.g. in case of a single hole in a t_{2g}-shell, the anisotropic orbital interactions as well as related frustration are transferred to pseudo-spin one-half Kramers doublets of d^5 ions [4, 11, 12]. However, in case of only partially lifting the degeneracy, the directional character of the electron density of the degenerate states is preserved, resulting in an effective reduction of magnetic sublattice dimensionality and strongly amplifying the effects of geometrical frustration. The Mott insulating d^1 double perovskites with undistorted cubic structure, such as spin-1/2 Ba_2BMoO_6 (B=Y,Lu) and Ba_2BOsO_6 (B=Na,Li), in which the only magnetically active ions, Mo^{5+} or Os^{7+}, reside on a weakly frustrated fcc sublattice well exemplify this physical scenario [13].

The osmium compounds Ba_2NaOsO_6 and Ba_2LiOsO_6 order magnetically [14–16]. Small effective local moments $\sim$0.7 μ_B, compared to spin only value 1.7 μ_B, have been extracted from high temperature susceptibilities in both materials [14]. The strong reduction of local moments is a direct manifestation of unquenched orbital momentum and strong SOC in the $5d$-shell of Os^{7+} ion [17–19]. In Ba_2NaOsO_6, anomalously small net ordered moment $\sim 0.2\mu_B$ has additionally been detected [15, 16]. Recent NMR measurements indicate a canted AF order in the Na compound [20].

The reported experimental data on Ba_2YMoO_6 are even more puzzling: this compound does not show any structural or magnetic transition down to 50 mK [21–23]. The total high temperature entropy extracted from electronic heat capacity was reported to be close to $R\ln 4$ [22], indicating the presence of an extra two-fold orbital degeneracy in addition to the spin, and allowing for the emergence of multi-orbital physics. Based on magnetic susceptibility and muon spin rotation data, a valence bond glass state, an amorphous arrangement of spin singlets, has been proposed for Ba_2YMoO_6 [22] which remains quite stable against isovalent substitutions of Ba^{2+} with Sr^{2+} [24]. The magnetic susceptibility of a very similar compound Ba_2LuMoO_6 also did not exhibit any magnetic transition down to 2 K [25]. Theoretically, various exotic phases, including multipolar order [13] and chiral spin-orbital liquid [26], have been put forward as possible candidates.

In this letter, we introduce and study a spin-orbital model and show that a dimer-singlet phase, composed of random arrangement of spin-orbit dimers, without any type of long-range order is a natural ground state of the model. The physical properties of this disordered phase are consistent with all available experimental findings on molybdenum double perovskites. In addition, the minimal model supports complex non-collinear, coplanar, ordered patterns. We argue that such four-sublattice ordered states are realised in osmium compounds.

Local electronic structure.– The single d-electron of

a Mo^{5+} or Os^{7+} ion in a cubic environment occupies t_{2g}-manifold of degenerate xy, xz, yz orbitals. It carries an effective angular momentum $l = 1$ with $|l^z{=}0\rangle \equiv |xy\rangle$, $|l^z{=}\pm1\rangle \equiv -\frac{1}{\sqrt{2}}(i|xz\rangle \pm |yz\rangle)$ [27]. The six-fold degeneracy of the local Hilbert space is lifted by the local SOC $H_{\rm so} = -\lambda \vec{l}\cdot\vec{S}$ stabilizing $j = l+S = \frac{3}{2}$ quartet and pushing $j = \frac{1}{2}$ Kramers doublet to a higher energy. Here, $\vec{S}$ is an electron spin operator and λ denotes the SOC. The states $j^z = \pm\frac{1}{2}$ of $j = \frac{3}{2}$ manifold have predominantly xy character, while $j^z = \pm\frac{3}{2}$ components are given by superposition of xz and yz orbitals only [see Fig. 1(a)]. When SOC is much smaller (larger) than the exchange interactions between neigbhoring ions, it is more convenient to use the t_{2g} ($j = \frac{3}{2}$) basis. The following analysis covers both limits.

Spin-orbital Hamiltonian.– In the double perovskite structure, each nearest-neighbor bond of the fcc sublattice of magnetic ions belongs to one of the crystallographic planes xy, xz, or yz as shown in Fig. 1(b). We label these bonds as well as the t_{2g}-orbitals with a cubic axis $\gamma(= a, b, c)$ normal to their planes, e.g. xy becomes c. The hopping between neighboring t_{2g}-orbitals takes place through intermediate oxygens' p-orbitals, or direct hybridization. Along a γ-type bond the dominant overlap, with amplitude t, is between γ-orbitals [13, 28]. The low-energy spin-orbital model is obtained via standard second order perturbation theory in t/U (U being the local Coulomb repulsion) [29], and reads as follows:

$$\mathcal{H} = \sum_{\langle ij\rangle_\gamma} \Big[-J_1\big(\vec{S}_i\cdot\vec{S}_j + \frac{3}{4}\big) + J_2\big(\vec{S}_i\cdot\vec{S}_j - \frac{1}{4}\big)\Big] P_{ij}^{(\gamma)} + J_3 \sum_{\langle ij\rangle_\gamma} \big(\vec{S}_i\cdot\vec{S}_j - \frac{1}{4}\big)\bar{P}_{ij}^{(\gamma)} - \lambda\sum_i \vec{l}\cdot\vec{S}\,. \qquad (1)$$

$\langle ij\rangle_\gamma$ denotes a γ-type bond, $J_{1(2)} = \frac{1}{4}Jr_{1(2)}$, $J_3 = \frac{1}{3}J(2r_2 + r_3)$, $J = 4t^2/U$, the set of r_n describing the multiplet structure of excited states are functions of $\eta = J_H/U \ll 1$ [30], and J_H is the Hund's coupling.

The isotropic spin exchange couplings depend on the orbital occupancy of the corresponding bonds [3, 31], and are described by the first three terms of Eq. (1), with the orbital projectors $P_{ij}^{(\gamma)} = n_i^{(\gamma)}(1-n_j^{(\gamma)}) + (1-n_i^{(\gamma)})n_j^{(\gamma)}$ and $\bar{P}_{ij}^{(\gamma)} = n_i^{(\gamma)}n_j^{(\gamma)}$, where $n_i^{(\gamma)}$ is the occupation number of a γ-orbital. The spin isotropy is broken by the SOC in Eq. (1), allowing symmetric anisotropic exchange between $j = \frac{3}{2}$ quartets. In cubic double perovskites, the antisymmetric Dzyaloshinsky-Moriya exchange is forbidden by the bond inversion symmetry.

Dimer-singlet phase.– We start our analysis by setting the small parameter $\eta = 0$, and discuss later the model (1) in its full parameter space. We consider two limiting cases when $\lambda \ll J$ or $\lambda \gg J$, and identify the ground state phases of the model (1) through analytical considerations. At $\eta = 0$, first three terms of the model (1) can be grouped, up to a constant term, into one [31], and the model simplifies to

$$\mathcal{H} = J\sum_{\langle ij\rangle_\gamma} \big(\vec{S}_i\cdot\vec{S}_j + \frac{1}{4}\big)\bar{P}_{ij}^{(\gamma)} - \lambda\sum_i \vec{l}\cdot\vec{S}\,. \qquad (2)$$

The expectation value of the first term in Eq. (2) in any classical, i.e. site-factorized, state is non-negative. At $\lambda = 0$, the zero minimum classical energy is achieved by forming decoupled layers of AF square lattices with uniform planar orbital order. In this state, the orbital projectors $\bar{P}_{ij}^{(\gamma)} = 1(0)$ on intra-(inter-)layer bonds and $\langle\vec{S}_i\cdot\vec{S}_j\rangle = -\frac{1}{4}$ on intra-layer bonds. Hence, orbital 'flavors' are decoupled and flipping locally an orbital 'flavor' does not cost energy, resulting in a massive ground state degeneracy [31]. A product state constructed from entangled quantum spin-orbit states on decoupled dimer bonds has however lower negative energy, $\mathsf{E}_{\rm DS} = -\frac{1}{4}J$. This phase, termed here as dimer-singlet phase, corresponds to a hard-core dimer covering of the fcc lattice, with $\bar{P}_{ij}^{(\gamma)} = 1(0)$ on (inter-)dimer bonds. On a dimer bond, spins form a singlet and occupied orbitals have lobes directed along the bond. Covering the lattice with such dimers is in fact an exact eigenstate of the Hamiltonian (2). When neighboring dimers are in the same plane, an energetically unfavorable larger clusters of AF coupled spins are formed [32], and such configurations are banned from the ground state manifold. Although, this seems to be a rather strong constraint, the orientational degeneracy of dimer covering remains extensive [31].

For $\lambda \gg J$, the t_{2g}-levels are split and the components of the lower $j = 3/2$ quartet forms the relevant basis, that we label by pseudo-spin $\vec{s}$ and pseudo-orbital $\vec{\tau}$ states: $|\tau^z = \frac{1}{2},\ s^z = \pm\frac{1}{2}\rangle \equiv |j = \frac{3}{2},\ j^z = \pm\frac{1}{2}\rangle$ and $|\tau^z = -\frac{1}{2},\ s^z = \pm\frac{1}{2}\rangle \equiv |j = \frac{3}{2},\ j^z = \pm\frac{3}{2}\rangle$ [33]. Projecting Eq. (2) onto this

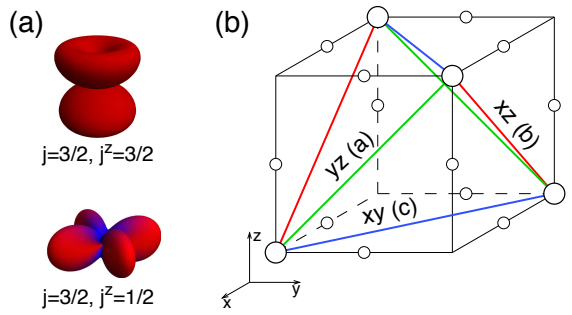

FIG. 1. (a) Density profile of $j = 3/2$ quartet. The states $j^z = \pm\frac{1}{2}$ (bottom) have dominant xy-orbital character, while $j^z = \pm\frac{3}{2}$ components (top) are composed of xz and yz orbitals. Red and blue coloring denotes the up and down spin distribution, respectively. (b) Crystallographic unit cell containing four molybdenum ions (large circles). Oxygen positions are indicated by small circles. The nearest-neighbor bonds belonging to different cubic planes are distinguished by different colors. The t_{2g}-orbitals active along the corresponding bonds are also indicated.

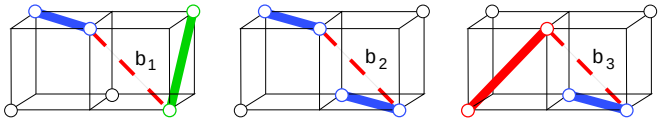

FIG. 2. Types of different inter-dimer bonds depicted as dashed lines. Dimers are represented with ○—○ and are colored according to three cubic planes they belong to. Bonds b_1 and b_2 couple dimers with perpendicular to these bonds. Bond b_3 connects a dimer from a orthogonal plane with another one that is in the same plane as b_3 itself.

new basis, we find

$$\mathcal{H} = \tilde{J} \sum_{\langle ij \rangle_\gamma} \big(\vec{s}_i \cdot \vec{s}_j + \frac{1}{4} \big) \tilde{P}_{ij}^{(\gamma)} \,, \tag{3}$$

where $\tilde{P}_{ij}^{(\gamma)} = (\frac{1}{2} + \tau_i^{(\gamma)})(\frac{1}{2} + \tau_j^{(\gamma)})$, $\tilde{J} = \frac{4}{9} J$, $\tau^{(a)} = -\frac{1}{2}\tau^z - \frac{\sqrt{3}}{2}\tau^x$, $\tau^{(b)} = -\frac{1}{2}\tau^z + \frac{\sqrt{3}}{2}\tau^x$, and $\tau^{(c)} = \tau^z$. Hamiltonian (3) has the same form as the Kugel-Khomskii model of e_g-orbitals on a cubic lattice [3] and explicitly reveals the emergent, at large λ, hidden SU(2) symmetry pointed out in Ref. 13. Similarly to $\lambda = 0$, the ground state manifold of (3) is spanned by dimer-singlets, but now these are composed of pseudo-spins instead of real spins.

Insight for intermediate λ can be gained by exactly solving the model (1) on an isolated bond, since the inter-dimer couplings appear to be much smaller than intra-dimer ones (see below). For each values of λ, we find the singlet ground state

$$|\bigcirc\!\!-\!\!\bigcirc\rangle = \big(|\Uparrow\Downarrow\rangle - |\Downarrow\Uparrow\rangle \big)/\sqrt{2} \,, \tag{4}$$

where the wave-functions of pseudo-spins $\Uparrow$ ($\Downarrow$) depend on the strength of λ [31], e.g., in the xy-plane, we have

$$|\Uparrow (\Downarrow)\rangle = \cos\vartheta \, |0, \uparrow (\downarrow)\rangle + \sin\vartheta \, |(-)1, \downarrow (\uparrow)\rangle \;. \tag{5}$$

In the two limiting cases, $\lambda = 0$ and $\lambda \gg 1$, the variational parameter θ becomes 0 and $\arccos\sqrt{\frac{2}{3}}$, respectively. The SOC inflates the planar orbital, so that at large λ it becomes $\big|j{=}\frac{3}{2}, j_z{=}\pm\frac{1}{2}\big\rangle$. The latter has small out-of-plane component, see Fig. 1(a), generating finite but small interactions between, otherwise decoupled, dimers. However, as it follows, inter-dimer couplings do not select any particular superstructure of dimers.

Fig. 2 shows all possible inter-dimer bonds allowed in the ground state manifold. Such a bond may connect two dimers both perpendicular the connecting bond itself: then, either the connected dimers belong to different planes (b_1) or to the same plane (b_2). The third possibility, b_3, is that one of the dimers is in the same plane as the inter-dimer bond, and the other is perpendicular to them [see Fig. 2]. Consequently, regardless of the dimer arrangements, each dimer has exactly six neighboring b_3 bonds. Out of $6\mathcal{N}$ bonds of the fcc lattice with $\mathcal{N}$ sites, there are in total $\frac{1}{2}\mathcal{N}$ dimer bonds, $3\mathcal{N}$ b_3-type, and remaining $\frac{5}{2}\mathcal{N}$ b_1 or b_2 type of bonds. Each dimer (b_n-type) bonds host a finite energy $\mathcal{E}_\mathsf{d}$ ($\mathcal{E}_{\mathsf{b}_n}$). As both b_1 and b_2 bonds connect dimers out of their plane, $\mathcal{E}_{\mathsf{b}_1} = \mathcal{E}_{\mathsf{b}_2}$ and the energy of a product dimer state

$$\mathsf{E}_{\mathsf{DS}} = \big(\mathcal{E}_\mathsf{d} + 5\mathcal{E}_{\mathsf{b}_1} + 6\mathcal{E}_{\mathsf{b}_3} \big) \mathcal{N}/2 \tag{6}$$

is independent of the dimer covering. Hence, the inter-dimer couplings do not order dimers and the massive orientational degeneracy persists. In real materials, however, a mis-site disorder and/or uncorrelated local distortions most likely select a random dimer covering, rendering the system to freeze in a glassy manner.

In an amorphous dimer-singlet phase, momenta of the excitations are not well defined, but their energies are. Moreover, the inter-dimer couplings are much smaller than the intra-dimer exchange, allowing isolated dimer description of the bulk magnetic spectra. At $\eta, \lambda = 0$, as product dimer states are exact eigenstates, spins of different dimers are completely decoupled. In the large λ limit, the inter-dimer pseudo-spin exchange $J' \simeq \frac{1}{16}\tilde{J} \ll \tilde{J}$. This estimate follows from Eq. (3) by noting that $\langle \tilde{P}_{ij}^{(\gamma)} \rangle = \frac{1}{16}$ on the inter-dimer bonds. Two types of local excitations allowed by magnetic dipole transitions are illustrated in Fig. 3. The upper one corresponds to flipping locally a (pseudo-)spin at the energy cost $\Delta_\mathrm{S} = J$ ($\tilde{J}$) in small (large) λ limit. The lower is a (pseudo-)orbital excitation that costs half the energy, $\Delta_\mathrm{O} = \frac{1}{2}J$ ($\frac{1}{2}\tilde{J}$), of a spin-like excitation. These estimates follow from the expectation values of the limiting Hamiltonians Eqs.(2,3) in the ground state of an isolated bond, Fig. 3(left), and its excited states, Fig. 3(right). Using reported parameters for Ba_2YMoO_6 [29], we estimate energy of spin-like (orbital-like) excitations $\Delta_{\mathrm{S(O)}} \simeq 20 - 45$ $(10 - 23)$ meV, for large−small SOC, and their bandwidth ($\sim J'$) of about few meV. In the magnetic dipolar channel, spin-like excitations carry stronger intensity than orbital-like ones. These findings agree well with neutron scattering data on powder samples discussed below.

There are additional thermally accessible non-local excitations at lower energies. For example AF coupled spin clusters, or orphan spins may emerge as a result of thermally induced orbital reorientation. An important difference between the well studied spin-only dimer systems and our model is the lack of a hard-gap. Here, on account of orbital degrees of freedom, the spectrum cannot be characterized by a single energy scale.

Phase diagram.– To explore the entire phase diagram of the full Hamiltonian (1), we used a site-factorized variational approach and compared the energies of ordered and dimer-singlet phases. The latter is numerically obtained from Eq. (6) using a product state of the exact wave-functions of isolated dimers. Within our variational approach, the magnetic and crystallographic unit cells

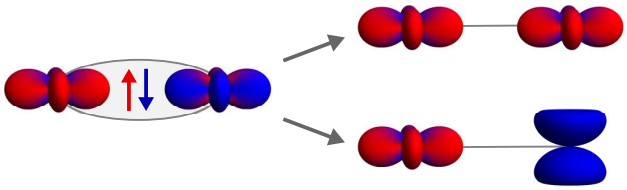

FIG. 3. Excitations of a spin-orbit dimer in the large λ limit. Flipping locally, for example, the $j^z = -1/2$ component to $j^z = 1/2$ or to $j^z = -3/2$ corresponds to flipping the pseudo-spin (top) or pseudo-orbital (bottom), respectively. Local excitations for small SOC correspond to changing the real spins or orbitals.

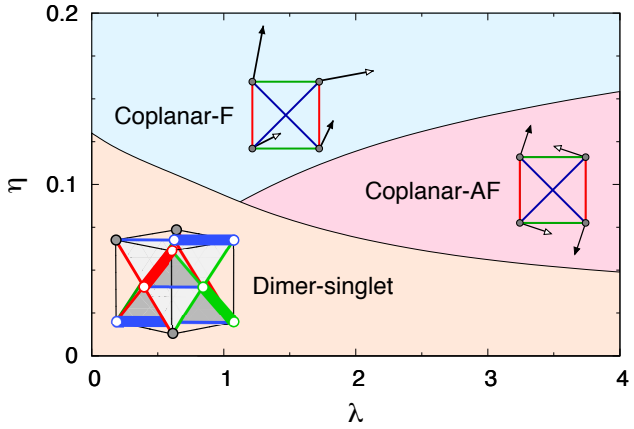

FIG. 4. Phase diagram of the model (1) as the function of Hund's coupling η and the SOC λ (in units of J). For small values of η the dimer-singlet phase (see inset) is stable over the entire range of λ. With increasing Hund's coupling, non-collinear coplanar phases with ordered moments in one of the cubic planes are stabilized. The ferro-type coplanar state, coplanar-F, has a finite net moment pointing along [110] (or equivalent) direction. The cartoon figures show a tetrahedron of four molybdenum sites projected onto the plane of ordered $\vec{j}$-moments, depicted as arrows.

coincide, however, we still need forty variational parameters to construct a trial wave-function [31]. When $\eta = 0$ the ground state is a random arrangement of spin-orbit dimers [see inset in Fig. 4] for any value of λ. Only the nature of pseudo-spins forming the singlet dimers is affected by λ, in accordance with the above analytical considerations. For large enough Hund's coupling, we find two non-collinear but coplanar phases of ordered total angular momenta $\vec{j}$ [see Fig. 4]. One, termed here as coplanar-F, has finite net moment along [110] (or equivalent) direction, i.e. along one of the NN bond, as experimentally observed [14]. The other, coplanar-AF, has no net moment. In the dimer-singlet phase, on a dimer bond in γ-plane corresponding γ-orbital is predominately occupied, with occupancy decreasing from $n^{(\gamma)} = 1$ to $\frac{2}{3}$ with increasing λ. Hunds coupling induced transitions to ordered states are accompanied by complex rearrangements of an electron density within SOC split t_{2g}-multiplet, with orbital occupancies dictated by the actual values of parameters, e.g. in coplanar-AF order in a cubic γ-plane the α- and β-orbitals are predominantly occupied compared to the in-plane γ-orbital. All phase boundaries appear to be first order within our approach: the net moment and the order parameters drop to zero across the transitions from coplanar-F to coplanar-AF state and from the ordered to disordered dimer-singlet phase, respectively. However, one cannot rule out a second order symmetry allowed transition between ordered states, or an exotic continuous transition from spontaneously dimerized phase to ordered states [34].

Experimental implications.– The dimer-singlet phase captures experimental observations on the molybdenum compounds. In agreement with experiments, it does not exhibit any long-range ordering nor breaks any global symmetry. Its extensive degeneracy explains the observed glassy behavior and suggest the presence of a residual entropy, that cannot be excluded based on heat capacity data [22]. Magnetic susceptibility and electronic heat capacity [22, 23] suggest the presence of pseudo-gapped, rather than hard-gapped, low-energy excitations, consistent with the dimer-singlet phase. Neutron scattering experiments on powder samples [35] revealed excitations that are in line with the spectrum of weakly coupled spin-orbit dimers. An intense 'mode' observed at $\Delta_S \simeq 28$ meV with bandwidth of about 4 meV is interpreted here as a (pseudo-)spin singlet-to-triplet excitation. A less intense, lower-energy ($\Delta_O \simeq 9 - 17$ meV) response centred around at half the energy of Δ_S is naturally attributed to (pseudo-)orbital excitation. These lower-lying excitations have also been observed in NMR response [21]. The energetics of the observed excitations agrees well with above estimates $\Delta_{S(O)} \simeq 20 - 45$ $(10 - 23)$ meV. In addition, the infrared transmission spectra indicate the emergence of uncorrelated local distortions of MoO_6 octahedra below 130 K [36], at around the same temperature the magnetic susceptibility start to decrease, most likely due to formation of spin-orbit dimers. In the dimer-singlet phase, such uncorrelated distortions emerge due to the directional character of the occupied orbitals.

The four-sublattice ordered states in the phase diagram (Fig. 4) may provide description for the iso-structural osmium compounds, Ba_2LiOsO_6 and Ba_2NaOsO_6. The latter is characterized by very small net magnetic moment $\sim 0.2\mu_B$ along [110] easy axis [14]. We find the net moment $\vec{M} = 2\vec{S} - \vec{l}$ along the same [110] (or equivalent) direction, being $\sim 1\mu_B$ for small and $\sim 0.1\mu_B$ for large λ.

To summarize, within a minimal microscopic model, we have proposed unified theoretical description of possible ground states in d^1 cubic double perovskites. The

obtained spin-orbital model shows a rich phase behavior including a massively degenerate dimer-singlet manifold, without any long-range order, and unusual non-collinear ordered patterns. Our theoretical study elucidates physics behind and provides explanations of experimental data on molybdenum and osmium based compounds. The physics discussed here may also be relevant to other heavy transition metal compounds, such as molybdenum pyrochlores, in which random distribution of 'dimerized' bonds, induced by orbital degrees, have been recently revealed by pair-distribution function measurements [37].

We thank G. Chen, M. Haverkort, G. Khaliullin, F. Mila, W. Natori, J.A.M. Paddison, S. Streltsov, and H. Takagi for discussions. J.R. acknowledges funding from the Hungarian OTKA grant K106047. L.B. was supported by the NSF Materials Theory program under grant NSF DMR1506119. G.J. benefitted from the facilities of the KITP, and was supported in part by the NSF under Grant No. NSF PHY11-25915.

* Also at Andronikashvili Institute of Physics, 0177 Tbilisi, Georgia

[1] L. Balents, Nature **464**, 199 (2010).
[2] L. Savary and L. Balents, ArXiv e-prints (2016), arXiv:1601.03742 [cond-mat.str-el].
[3] K. Kugel and D. Khomskii, Sov. Phys. Usp. **25**, 231 (1982).
[4] G. Khaliullin, Prog. Theor. Phys. Suppl. **160**, 155 (2005).
[5] H. F. Pen, J. van den Brink, D. I. Khomskii, and G. A. Sawatzky, Phys. Rev. Lett. **78**, 1323 (1997).
[6] G. Khaliullin and S. Maekawa, Phys. Rev. Lett. **85**, 3950 (2000).
[7] F. Vernay, K. Penc, P. Fazekas, and F. Mila, Phys. Rev. B **70**, 014428 (2004).
[8] S. Di Matteo, G. Jackeli, C. Lacroix, and N. B. Perkins, Phys. Rev. Lett. **93**, 077208 (2004).
[9] S. Di Matteo, G. Jackeli, and N. B. Perkins, Phys. Rev. B **72**, 024431 (2005).
[10] G. Jackeli and D. Khomskii, Phys. Rev. Lett. **100**, 147203 (2008).
[11] G. Chen and L. Balents, Phys. Rev. B **78**, 094403 (2008).
[12] G. Jackeli and G. Khaliullin, Phys. Rev. Lett. **102**, 017205 (2009).
[13] G. Chen, R. Pereira, and L. Balents, Phys. Rev. B **82**, 174440 (2010).
[14] K. Stitzer, M. Smith, and H.-C. zur Loye, Solid State Sciences **4**, 311 (2002).
[15] A. Erickson, S. Misra, G. Miller, R. Gupta, Z. Schlesinger, W. Harrison, J. Kim, and I. Fisher, Phys. Rev. Lett. **99**, 016404 (2007).
[16] A. Steele, P. Baker, T. Lancaster, F. Pratt, I. Franke, S. Ghannadzadeh, P. Goddard, W. Hayes, D. Prabhakaran, and S. Blundell, Phys. Rev. B **84**, 144416 (2011).
[17] K.-W. Lee and W. E. Pickett, Europhys. Lett. **80**, 37008 (2007).
[18] S. Gangopadhyay and W. Pickett, Phys. Rev. B **91**, 045133 (2015).
[19] S. Gangopadhyay and W. E. Pickett, Phys. Rev. B **93**, 155126 (2016).
[20] L. Lu, M. Song, W. Liu, A. P. Reyes, P. Kuhns, H. O. Lee, I. R. Fisher, and V. F. Mitrović, Nature Communications **8**, 14407 EP (2017).
[21] T. Aharen, J. Greedan, C. Bridges, A. Aczel, J. Rodriguez, G. MacDougall, G. Luke, T. Imai, V. Michaelis, S. Kroeker, H. Zhou, C. Wiebe, and L. Cranswick, Phys. Rev. B **81**, 224409 (2010).
[22] M. de Vries, A. Mclaughlin, and J.-W. Bos, Phys. Rev. Lett. **104**, 177202 (2010).
[23] M. de Vries, J. Piatek, M. Misek, J. Lord, H. Rnnow, and J.-W. G. Bos, New Journal of Physics **15**, 043024 (2013).
[24] A. Mclaughlin, M. de Vries, and J.-W. Bos, Phys. Rev. B **82**, 094424 (2010).
[25] F. Coomer and E. Cussen, Journal of Physics: Condensed Matter **25**, 082202 (2013).
[26] W. Natori, E. Andrade, E. Miranda, and R. Pereira, Phys. Rev. Lett. **117**, 017204 (2016).
[27] A. Abragam and B. Bleaney, *Electron Paramagnetic Resonance of Transition Ions* (Clarendon Press, Oxford, 1970).
[28] Recent *ab-initio* study of Ba_2YMoO_6 suggests $t \simeq 0.15$ eV and order of magnitude smaller NN off-diagonal as well as further neighbor hopping amplitudes, S. Streltsov (privet communication).
[29] The parameters $t \simeq 0.12 - 0.15$ eV [15, 28] and $U \simeq 2 - 3$ eV [15, 38] have been suggested for molybdenum and osmium double perovskites. We thus estimate $t/U \sim 0.04-0.07$ that is small enough to justify our perturbative t/U expansion up to the leading order.
[30] $r_1 = 1/(1-3\eta)$, $r_2 = 1/(1-\eta)$ and $r_3 = 1/(1+2\eta)$.
[31] See supplemental material at [URL] for the details.
[32] G. Jackeli and D. A. Ivanov, Phys. Rev. B **76**, 132407 (2007).
[33] Similar representation has been used in Ref. 26.
[34] T. Senthil, A. Vishwanath, L. Balents, S. Sachdev, and M. P. A. Fisher, Science **303**, 1490 (2004).
[35] J. P. Carlo, J. P. Clancy, T. Aharen, Z. Yamani, J. P. C. Ruff, J. J. Wagman, G. J. Van Gastel, H. M. L. Noad, G. E. Granroth, J. E. Greedan, H. A. Dabkowska, and B. D. Gaulin, Phys. Rev. B **84**, 100404 (2011).
[36] Z. Qu, Y. Zou, S. Zhang, L. Ling, L. Zhang, and Y. Zhang, Journal of Applied Physics **113**, 17E137 (2013).
[37] P. M. M. Thygesen, J. A. M. Paddison, R. Zhang, K. A. Beyer, K. W. Chapman, H. Y. Playford, M. G. Tucker, D. A. Keen, M. A. Hayward, and A. L. Goodwin, Phys. Rev. Lett. **118**, 067201 (2017).
[38] L. Vaugier, H. Jiang, and S. Biermann, Phys. Rev. B **86**, 165105 (2012).